

Self-assembled InSb and GaSb quantum dots on GaAs(001)

B.R. Bennett, P.M. Thibado, M.E. Twigg, E.R. Glaser, R. Magno,
B.V. Shanabrook, and L.J. Whitman
Naval Research Laboratory, Washington, DC 20375-5347

(Received 18 September 1995; accepted 4 December 1995)

Quantum dots of InSb and GaSb were grown on GaAs(001) by molecular-beam epitaxy. *In situ* scanning tunneling microscopy measurements taken after 1–2 monolayers of InSb or GaSb growth reveal the surface is a network of anisotropic ribbon-like platelets. These platelets are a precursor to quantum dot growth. Transmission electron microscopy measurements indicate that the quantum dots are coherently strained. Quantum dots of InSb and GaSb capped by GaAs exhibit strong luminescence near 1.1 eV.

I. INTRODUCTION

Strain-induced islands form during heteroepitaxy in many material systems. Under appropriate growth conditions, these islands are coherent, isolated, and sufficiently small to exhibit electron confinement properties. These coherent islands or “quantum dots” (QDs) are said to be self-assembled because no lithographic patterning is required. Furthermore, it may be possible to find a material system and growth conditions to form ensembles of nearly identical QDs. If such a process can be invented, the electronic and optical properties of the QDs will exhibit little inhomogeneous broadening, making them ideal for use in applications such as solid-state lasers and resonant tunneling devices.

In the last three years, several groups have produced InAs quantum dots embedded in GaAs using molecular beam epitaxy (MBE) or organometallic vapor phase epitaxy. In addition, self-assembled QDs have been produced in other arsenide- and phosphide-based heterostructures.¹ Recently, we reported the growth of InSb, GaSb, and AlSb QDs on GaAs.^{2,3} Hatami *et al.* also investigated GaSb QDs,⁴ and Watanabe *et al.* fabricated InSb QDs on Se-terminated GaAs.⁵ For all three Sb-based materials, we determined growth conditions which yielded Stranski-Krastanov growth, with the first 1–3 monolayers (ML) forming a 2D wetting layer, followed by the strain-induced formation of QDs. We found the onset of dot formation to occur after approximately 1.5 ML InSb or 2.5 ML GaSb, although these values may be a function of several variables including substrate temperature, surface reconstruction, growth rate, and anion flux. In this paper, we investigate the formation of InSb and GaSb QDs on GaAs by transmission electron microscopy (TEM), atomic force microscopy (AFM), photoluminescence (PL), and *in situ* scanning tunneling microscopy (STM). We show that the formation of platelets is a precursor to QD formation. TEM measurements and strong luminescence indicate that the QDs are coherently strained.

II. EXPERIMENT

Samples were grown by solid-source MBE on semi-insulating (SI) substrates, nominally oriented within 0.1° of (001). Growth temperatures were determined by measuring the absorption edge of the substrate via infrared transmission

thermometry.⁶ First, a GaAs buffer layer, 0.5–1.0 μm thick, was grown at 580°C with interrupts and a growth rate of 1.0 ML/s. Growth was monitored by reflection high-energy electron diffraction (RHEED). During the GaAs buffer growth, the RHEED pattern is a streaky (2×4) reconstruction with no evidence of transmission spots. Before the growth of the dots, a 450 s growth interrupt under an As_4 flux was performed, resulting in sharp diffraction spots along each streak, indicating the formation of large terraces. After the interrupt, the substrate temperature was reduced, the valve for the arsenic source was closed to minimize As incorporation, and the antimonide layer was grown by migration-enhanced epitaxy (MEE) with a cation deposition rate of 0.10 ML/s and a V:III flux ratio of approximately 2:1. After deposition of the (In,Ga)Sb monolayers, the sample was held at the growth temperature under an Sb flux for 140 s before cooling. For example, to grow 2.0 ML of InSb, the shutter sequence is: 5 s In, 20 s Sb, 5 s In, 20 s Sb, 5 s In, 20 s Sb, 5 s In, 140 s Sb. Selected samples were capped with GaAs to protect the QDs from oxidation.

All samples were characterized by AFM using Park Scientific SiN_x cantilevers or Si ultraleversTM under ambient conditions. Selected samples were transferred under ultra-high vacuum (UHV) conditions to an UHV STM chamber, and imaged in constant-current mode (sample bias of -2.0 V, current of 0.1 to 0.5 nA). Samples were also examined by TEM after ion milling at 77 K. We characterized capped heterostructures by low-temperature PL, using the 488 nm line from an Ar^+ laser and a Ge detector cooled to 77 K.

III. RESULTS AND DISCUSSION

AFM and STM measurements of GaAs homoepitaxial layers prior to antimonide deposition reveal large terraces ($\sim 0.3 \mu\text{m}$) separated by 3 Å height (ML) steps. The surface morphology is very different after growth of 1.5–2.0 ML of InSb at 400 °C, as shown by the STM images in Fig. 1. After 2.0 ML, the surface includes a high density of QDs ($\sim 7 \times 10^8/\text{cm}^2$) with typical dot dimensions of height=8 nm and diameter=110 nm, as shown in Fig. 1(a). Ambient AFM measurements (using SiN_x tips) on the same sample yielded a similar height, 8.2 ± 0.5 nm, but a smaller diameter, 76 ± 7 nm. It is not surprising that the measured diameters are dif-

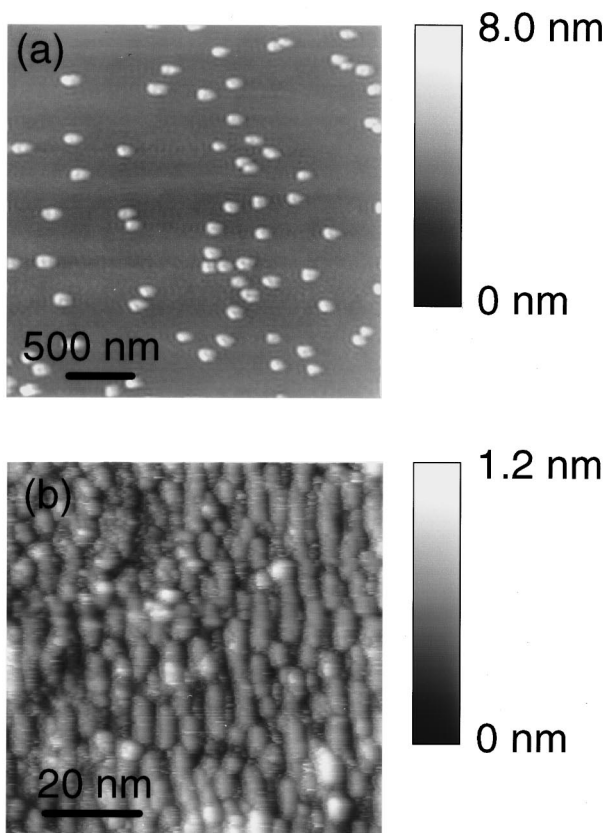


FIG. 1. *In situ* scanning tunneling microscopy images of InSb on GaAs(001): (a) 2.0 ML InSb, 3 μm by 3 μm , (b) 1.5 ML InSb, 80 nm by 80 nm.

ferent because the apparent QD size and shape is actually a convolution of the QD and the geometry of either an STM or AFM tip. Additional AFM measurements were performed on a different area of the same sample with both SiN_x and Si tips (the Si tips have a larger aspect ratio). The results were: SiN_x tip, height= 5.5 ± 0.9 nm, diameter= 72 ± 15 nm; Si tip, height= 5.1 ± 0.6 nm, diameter= 77 ± 14 nm. In addition, these QDs were imaged by scanning electron microscopy (SEM) which found diameters of 67 ± 13 nm. In summary, we observe substantial variations in dot size across the sample. In a fixed area on the sample, AFM with either type of tip and SEM give comparable values for dot diameter.

QDs were also present after 1.5 ML InSb. Higher magnification STM images of an area with no QDs reveal a network of platelets (anisotropic ribbonlike ML-height islands separated by vacancy arrays) of about 5 nm width, as shown in Fig. 1(b). We have also observed similar platelets of GaSb on GaAs by *in situ* STM.⁷ The formation of a type of platelets as a precursor to QD growth was recently suggested in the theory of Priester and Lannoo, who showed that the existence of platelets could explain the relatively narrow size distribution of the QDs observed in the InAs/GaAs system.⁸ In their model, the first ML forms a continuous 2D film whereas the next 0.4 ML grows as a random spatial distribution of large, single-sized ML-height islands which, upon further growth, transform into uniformly sized QDs. We do not observe these large 2D islands.

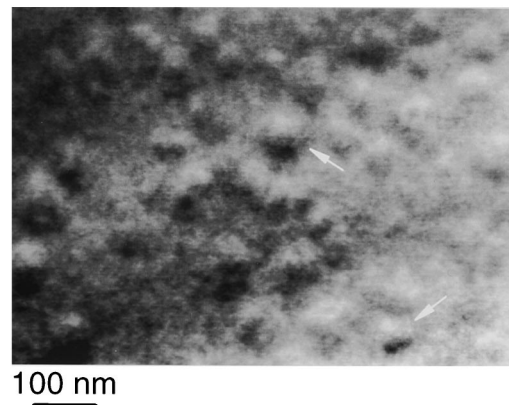


FIG. 2. Plan-view transmission electron microscopy image of 2.0 ML InSb on GaAs(001), collected with the diffraction vector $g=[220]$. Several quantum dots appear as bright features approximately 30 nm in diameter; two are indicated by arrows.

Many potential applications require QDs which are coherently strained and free of dislocations. Our STM and AFM measurements may not be sensitive to dislocations. Plan-view TEM measurements, however, can detect Moiré fringes which result from the difference in lattice constant between the substrate and an incoherent QD. Moiré fringes have been observed for dislocated InAs QDs.⁹ A plan-view TEM image of a 2 ML film of InSb grown at 430 $^\circ\text{C}$ is shown in Fig. 2. Several QDs, visible as bright features approximately 30 nm in diameter, are present but Moiré fringes are not, suggesting that the QDs are coherent. In contrast, Moiré fringes were observed on an InSb QD sample which exhibited anomalously shaped QDs in AFM.

For *ex situ* characterization, capped layers may be required to prevent oxidation of QDs. In some cases, however, the deposition of the cap may alter or destroy the QDs.^{10,11} To minimize the effect of cap growth on GaSb QDs, we deposited 3 ML GaSb at 490 $^\circ\text{C}$, followed by a 30 nm GaAs cap using MEE at 410 $^\circ\text{C}$. Plan-view and cross-sectional

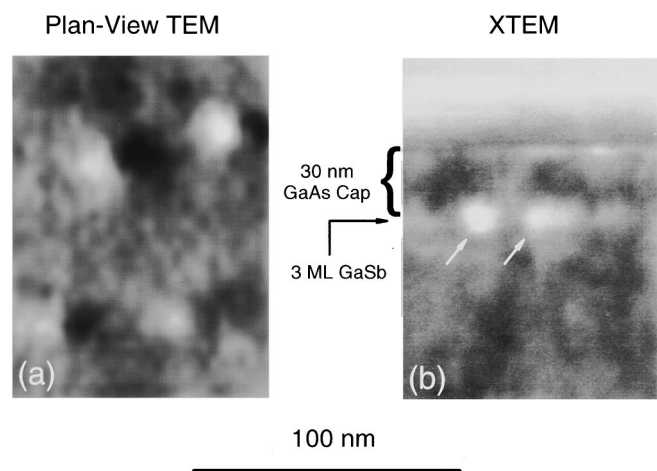


FIG. 3. Transmission electron microscopy images of 3.0 ML GaSb on GaAs(001), capped with 30 nm GaAs: (a) plan-view with $g=[220]$; (b) cross-sectional with $g=[200]$, and two quantum dots indicated by arrows.

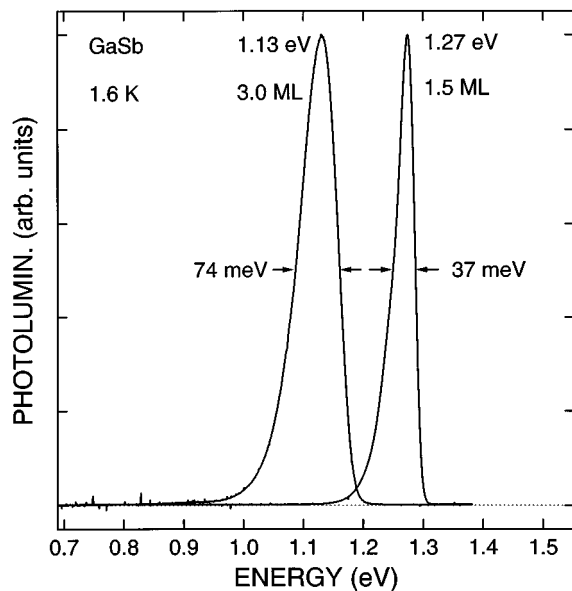


FIG. 4. Photoluminescence of GaAs-capped GaSb layers measured at 1.6 K with a power density of 2.8 W/cm^2 . The peak intensities are normalized in this plot; the integrated intensities for the two samples were approximately equal.

TEM images are shown in Fig. 3. Four QDs are present in the plan-view TEM image, shown in Fig. 3(a). We observe no evidence of Moiré fringes, suggesting that the QDs are coherent. The cross-sectional image [Fig. 3(b)] shows two QDs. Both plan-view and cross-sectional images indicate QD dimensions are on the order of 10 nm. AFM measurements of an uncapped 3 ML GaSb sample with similar growth parameters yielded an average QD height of 3.3 nm and diameter of 28 nm. Differences between TEM and AFM measurements may result from three effects: changes induced in the dot geometry by the GaAs cap, the fact that TEM is imaging strain fields associated with QDs, and tip-sample convolution in AFM.

The PL data for the capped 3 ML GaSb sample are plotted in Fig. 4, along with a GaAs-capped 1.5 ML GaSb sample. Based upon AFM and STM of uncapped samples as well as RHEED patterns during growth, we do not expect QDs for the 1.5 ML sample. The relatively narrow peak for the 1.5 ML coverage probably results from the 2D wetting layer of GaSb embedded in GaAs. Compared to the 1.5 ML sample, the luminescence for 3.0 ML GaSb is 140 meV lower in energy, a factor of two larger in peak width, and of equal integrated intensity. Peak broadening may reflect luminescence from QDs of different sizes, but additional work is required to confirm this hypothesis. The fact that the PL intensity was strong at 3.0 ML provides further evidence that the critical thickness for dislocation formation in the QDs has not been reached.¹² We also note that our PL data are similar to that of Hatami *et al.* for GaSb/GaAs structures.⁴ The major difference is that they observed two PL peaks for a sample with QDs, and attributed the higher energy peak to

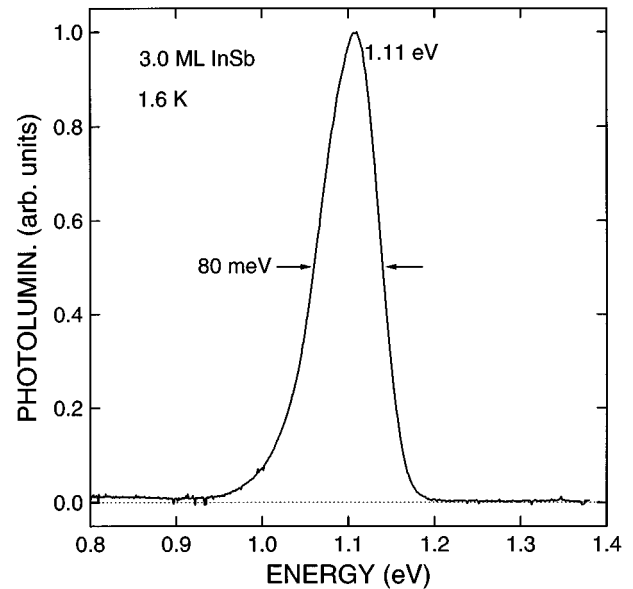


FIG. 5. Photoluminescence of GaAs-capped 3.0 ML InSb layer measured at 1.6 K with a power density of 2.8 W/cm^2 .

the 2D wetting layer. Our observation of only a single peak suggests that all the carriers are diffusing from the wetting layer into the QDs before recombining. Perhaps for the Hatami *et al.* sample the diffusion lengths of electrons and holes are smaller than the typical distance between QDs. We note that our PL results for GaSb QDs are qualitatively similar to measurements of InAs QDs in GaAs.¹² In the case of InAs/GaAs QDs, either one or two peaks can be observed depending on the growth conditions.^{13,14}

We also observed strong PL from an InSb QD sample consisting of 3.0 ML InSb capped by 20 nm GaAs. This cap was grown by MEE at 310°C because InSb is known to be unstable under an As flux above 320°C .¹⁵ The PL intensity peaks at an energy of 1.11 eV with a full width at half-maximum of 80 meV, as shown in Fig. 5.

The PL bands from both the GaSb^{4,16} and InSb¹⁶ QDs shift to higher energy with increasing excitation power density. In contrast, the PL energy for In(Ga)As QDs is nearly independent of excitation power density.^{16,17} These results suggest that the band alignment for GaSb and InSb QDs is type II, with electrons in the GaAs and holes in the GaSb or InSb. At high power densities, the Hartree potential shifts the relative energies of the electron and hole states and causes a shift of the PL to higher energy. The appropriate band structures for InSb/GaAs and GaSb/GaAs QDs are not known but are expected to be a strong function of both strain and confinement. This makes it difficult to derive a simple expression for the peak energy and indicates the need for a detailed calculation to predict energy levels of the QDs.

In summary, we have grown self-assembled GaSb and InSb quantum dots on GaAs by MBE. *In situ* STM measurements reveal that the formation of platelets is a precursor to

QD nucleation. The heterostructures with QDs are coherently strained and exhibit strong luminescence near 1.1 eV.

ACKNOWLEDGMENTS

The authors thank L. Ardis, P.B. Klein, R.J. Wagner, and J.R. Waterman for technical assistance. This work was sponsored by the Office of Naval Research and an NRC-NRL postdoctoral fellowship (P.M.T.).

¹P.M. Petroff and S.P. DenBaars, *Superlattice Microstruct.* **15**, 15 (1994), and references therein.

²B.R. Bennett, R. Magno, and B.V. Shanabrook, *Appl. Phys. Lett.* **68**, 505 (1996).

³B.R. Bennett, B.V. Shanabrook, and R. Magno, *Appl. Phys. Lett.* **68**, 958 (1996).

⁴F. Hatami *et al.*, *Appl. Phys. Lett.* **67**, 656 (1995).

⁵Y. Watanabe, T. Scimeca, F. Maeda, and M. Oshima, *Jpn. J. Appl. Phys.* **33**, 698 (1994).

⁶B.V. Shanabrook, J.R. Waterman, J.L. Davis, and R.J. Wagner, *Appl. Phys. Lett.* **61**, 2338 (1992).

⁷P.M. Thibado, B.R. Bennett, M.E. Twigg, B.V. Shanabrook, and L.J. Whitman, *J. Vac. Sci. Technol. A* **14**, 1607 (1996).

⁸C. Priester and M. Lannoo, *Phys. Rev. Lett.* **75**, 93 (1995).

⁹A. Madhukar, Q. Xie, P. Chen, and A. Konkar, *Appl. Phys. Lett.* **64**, 2727 (1994).

¹⁰X.W. Lin, Z. Liliental-Weber, J. Washburn, E.R. Weber, A. Sasaki, A. Wakahara, and Y. Nabetani, *J. Vac. Sci. Technol. B* **12**, 2562 (1994).

¹¹Q. Xie, P. Chen, A. Kalburge, T.R. Ramachandran, A. Nayfonov, A. Konkar, and A. Madhukar, *J. Cryst. Growth* **150**, 357 (1995).

¹²Y. Nabetani, N. Yamamoto, T. Tokuda, and A. Sasaki, *J. Cryst. Growth* **146**, 363 (1995).

¹³D. Leonard, M. Krishnamurthy, S. Fafard, J.L. Merz, and P.M. Petroff, *J. Vac. Sci. Technol. B* **12**, 1063 (1994).

¹⁴J.M. Gerard, J.B. Genin, J. Lefebvre, J.M. Moison, N. Lebouche, and F. Barthe, *J. Cryst. Growth* **150**, 351 (1995).

¹⁵M. Yano, H. Yokose, Y. Iwai, and M. Inoue, *J. Cryst. Growth* **111**, 609 (1991).

¹⁶E.R. Glaser, B.R. Bennett, B.V. Shanabrook, and R. Magno, *Appl. Phys. Lett.* (submitted).

¹⁷S. Fafard, R. Leon, D. Leonard, J.L. Merz, and P.M. Petroff, *Phys. Rev. B* **52**, 5752 (1995).